

# Biomechanical comparison of a transiliac internal fixator and two iliosacral screws in transforaminal sacral fractures: a finite element analysis

MARTIN SALÁŠEK<sup>1,2\*</sup>, MAGDALENA JANSOVÁ<sup>2</sup>, JIŘÍ KŘEN<sup>2</sup>,  
TOMÁŠ PAVELKA<sup>1</sup>, DRAHOMÍRA WEISOVÁ<sup>1,2</sup>

<sup>1</sup> Department of Orthopaedics and Traumatology,  
Faculty of Medicine of Charles University and Faculty Hospital in Plzeň, Czech Republic.

<sup>2</sup> Department of Mechanics, Faculty of Applied Sciences and New Technologies for Information Society  
of West Bohemian University in Plzeň, Czech Republic.

**Purpose:** Vertically unstable sacral transforaminal fractures can be stabilized with a transiliac internal fixator (TIFI) or two iliosacral screws (IS). This study was designed to compare stiffness between TIFI and IS. **Methods:** Using CT images finite element model of the pelvis was developed. Denis II type fracture was simulated and fixed either with TIFI or two IS. The sacral base was loaded vertically (250–500 N), displacement magnitudes on medial and lateral fracture surface and the maximum bone stress were calculated. The intact pelvis was used as a reference. Stiffness was determined by linear regression of load and displacement, computed stiffness ratio %. The von Mises stress was expressed as % ratio, evaluation of colour mapping was made. **Results:** The mean stiffness ratio medially in TIFI was 75.22%, in IS 46.54% ( $p = 0.00005$ ), laterally in TIFI 57.88%, in IS 44.74% ( $p = 0.03996$ ). The von Mises stress ratio of TIFI was 139.27%, of IS 565.35% ( $p < 0.00001$ ). **Conclusions:** Significantly higher stiffness and lower stress were found in TIFI model. TIFI provides a lower risk of over-compression of the fracture line in comparison with IS. TIFI thus exhibits superiority for fixation of transforaminal fractures, particularly with comminutive zone.

*Key words:* finite element analysis, transiliac internal fixator, iliosacral screw, pelvic ring, transforaminal fracture

## 1. Introduction

Unstable pelvic ring injuries are serious trauma at any age. High-energy mechanism of injury plays the main role in their etiology [2]–[6], [13], [16]. It is necessary to perform stabilization of the dorsal segment in completely unstable pelvic ring injuries [5], [6], [12], [13]. Minimally invasive internal fixation enables an acute stabilization of the posterior segment which is necessary not only to achieve hemodynamic stability, but also to allow early mobilization of the patient.

A transiliac internal fixator (TIFI) was first described by Füchtmeier in 2004 [6], iliosacral screw-

ing is a well established method of minimally invasive fixation of the posterior segment. TIFI is implanted in the prone position into the dorsal part of the iliac bone near the superior posterior iliac spine, and therefore is associated with a minimal risk of iatrogenic neurovascular injury [3], [6], [8], [10], [11], [17]. Conversely IS is inserted from the lateral surface of the iliac wing to the segment S1 or S2, which is associated with a significant risk of injury to the superior gluteal artery, respectively nerve roots L5, S1 and S2. The risk of iatrogenic injury is reduced in navigational techniques, due to the more accurate implantation of screws [7], [9], [14], [15], [18]–[21].

\* Corresponding author: Martin Salášek, Department of Orthopaedics and Traumatology, Faculty of Medicine of Charles University and Faculty Hospital, Alej Svobody 80, 304 60 Plzeň, Czech Republic. Tel: +420 37 745 1408, e-mail: martin.salasek@seznam.cz

Received: March 10th, 2014

Accepted for publication: June 2nd, 2014

The aim of the study was to compare the biomechanical stability of a transiliacal internal fixator and two iliosacral screws in internal fixation of vertically unstable transforaminal fracture.

## 2. Materials and methods

### 2.1. Creating a finite element model

A 3D model of the pelvis was created from 2D CT scans of the pelvis (thickness 0.8 mm). CT of the pelvis was performed as the content of the emergent whole-body CT in patient after vehicle accident, this pelvis was without any injuries. Normal bone marrow density was measured in this CT. The patient had body mass index 23.7 (weight 71 kg, height 1.73 m). The triangular surface mesh of the model was created from CT scans of a physiological female pelvis using specialized software. The pelvis was created as symmetrical. The 3D tetrahedral mesh was generated in Visual-Mesh software. The coccyx is not included in the model because it does not influence significantly the mechanical behaviour of the pelvis, simulation of pelvic floor muscles was not included in the model. The symphysis is modelled by solid tetrahedral elements with material properties taken from [1]. Uninjured SI joints were considered as a rigid structure, as a simplification the corresponding areas of the sacrum and hip bones were attached to each other by forming a rigid body.

The bones consist of a softer trabecular tissue covered by a stiffer compact tissue. The trabecular tissue is modelled by tetrahedral solid elements. A layer of triangular shell elements with 3 mm thickness is used for the compact tissue. The material properties of compact and trabecular bone (Young's modulus and Poisson's ratio) are taken from available literature – Bodzay et al. [1]. The head of the femur was replaced by a rigid body formed from a copied inner area of the acetabulum which was scaled slightly down. Sliding contact was defined between the head of the femur and the acetabulum. The femoral heads were virtually fixed in all degrees of freedom (translation ( $x, y, z$ ) and rotation ( $\alpha, \beta, \gamma$ )). The  $x$ -axis was determined in the medial-lateral direction, the  $y$ -axis in the anterior-posterior direction and the  $z$ -axis was in the caudal-cranial direction.

A model of the intact pelvis was created first, with the physiological position of both posterior segments without fractures and ligament disruption, this model

was used for comparison with other models. Then unilateral complete vertical transforaminal fracture (Denis II) together with complete symphyseolysis was created to simulate injury 61–C1.3 according to the AO classification. The disrupted pelvic ring was stabilized either with the transiliacal internal fixator or two iliosacral screws. For validation of the intact pelvic model, the plastic pelvis by Sawbones (number 1302, the full female pelvis with normal anatomy, made of the solid foam, a diameter of the acetabulum 48 mm) was used. This model was also loaded to the sacral base (linearly increasing the load from 250 N to 500 N). Measurement of displacements in  $x, y$  and  $z$  axes was performed by contactless stereo-photometric system in the visible light spectrum, evaluation of partial displacement and displacement magnitude was done in original analytic software by NTIS. There were the same regions of interest as in the finite element model (the sacral base, S1, S2, S3, S4 foramen). The finite element model for comparison with the plastic model was created of 2D CT scans of this model, therefore the shape and dimensions of both models were the same. Average measured values of displacement and values of displacement obtained from the finite element model were in good accordance, which allowed the finite element model to be used for further computing and other finite element models to be created.

In the case of TIFI, simulation was performed with a 3D model of TIFI, composed of tetrahedral elements. 7.5 mm polyaxial screws Legacy Medtronic<sup>®</sup> and a 6 mm transverse connecting rod were used, the lengths of screws and rod were adjusted to fit into the pelvic model, the entry point of screw was found in the region of the posterior superior iliac spine, the threaded part of the screw was deviated 30 degrees in sagittal plane and the tip of this screw was targeted to the supraacetabular part of the iliac bone.

The iliosacral screw is modelled by attaching together the nodes at the fracture area where the screw would be located. The attachment area has circular shape with approximately 4.5 mm in diameter. Two iliosacral screws were virtually inserted to the central zone of the first sacral segment through dorsal part of the iliac wing, the position of screws was confirmed on the sagittal scan on medial and lateral fracture surface. Two cannulated partially threaded screws Synthes<sup>®</sup>, 7.3 mm in diameter were used for simulation, the length of screws was also adjusted to fit into the model (the medial end of the screw thread was placed in the central sacral zone). Symphyseolysis was stabilized with a six-hole plate (3+3 cortex screws 3.5 mm, low profile 3.5 mm symphyseal plate, Synthes<sup>®</sup>).

However, further analysis of the pubic symphysis was not performed and the symphyseal plate was not visualized in the colour maps.

The sacral base was loaded by 500 N, corresponding to the standing upright position [1].

The load had vertical direction to the sacral base, initially as a preload 250 N was applied and then the load was being increased by 25 N up to 500 N linearly, the time between initial preload and full loading was 220 ms (Fig. 1). There was simulated the physiological load distribution in the sacral base, 80% load was transferred to the central part of the sacral base (articulation surface for the intervertebral disc L5/S1) and 20% was addressed to the facet joints of the S1 segment (for articulation of the inferior articular process of the vertebra L5).

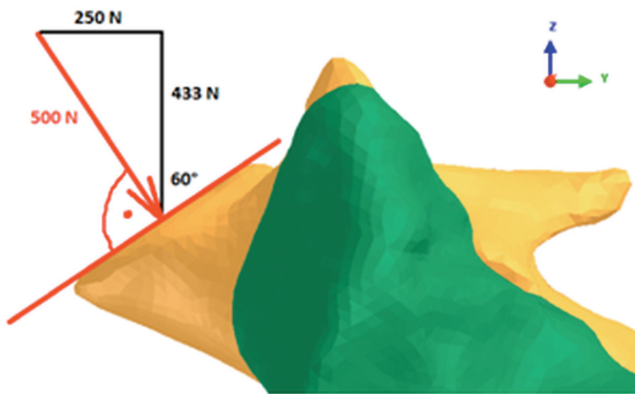


Fig. 1. The direction of load on sacral base and its distribution in  $y$ - and  $z$ -axis

## 2.2. Method of computing displacement magnitude, stiffness and the von Mises stress ratio

The models of TIFI and IS were tested for the aforementioned vertical load and the von Mises stress [MPa] and displacement in the fracture line [mm] was computed.

In the case of displacement displacement movements were measured in the selected nodes in the direction of  $x$ ,  $y$  and  $z$  axes (partial displacement in the direction of the axis) and the displacement magnitude, which in the case of measured displacements of node A  $x_A$ ,  $y_A$ ,  $z_A$  is determined as:  $l_A = \sqrt{x_A^2 + y_A^2 + z_A^2}$ . All models had graphic output in the form of colour mapping as well as data in the form of a graph of dependence of the displacement magnitude and load, or the von Mises stress on load, respectively. Linear dependence of data

was confirmed by the determination coefficient  $R^2$  (calculated in MS Excel<sup>®</sup>).

The inverse graph to load, depending on the displacement magnitude determined stiffness of TIFI and 2 IS, which were compared with the results of the model of intact pelvis. Stiffness was determined by linear regression analysis as the size of the load, depending on the displacement magnitude. The data was calculated as stiffness ratio in %, in TIFI was determined by the relation:  $stiffness\ ratio\ (TIFI) = \frac{k_{TIFI}}{k_0} \cdot 100$ , where  $k_{TIFI}$

is the stiffness determined in TIFI model and  $k_0$  is the stiffness of the intact pelvis (no fracture). In the IS model the calculation was:  $stiffness\ ratio\ (IS) = \frac{k_{IS}}{k_0} \cdot 100$ , where  $k_{IS}$  is the stiffness of model with two

iliosacral screws. During regression analysis a 95% confidence interval (95% CI) was also computed.

Data were obtained in the finite elements, which were located in the following areas: the central part of the base (B), the caudal edge of the foramen of S1 in the transforaminal fracture line (1), the caudal edge of the foramen S2 in the fracture line (2), in the caudal region of the foramen S3 (3) and also foramen S4 (4). In the area of S1 to S4 two nodes were always analyzed: the lateral surface of the fracture lines were identified as fracture (F, the portion of the fracture line closer to the transalar zone), on the medial surface of the fracture line as the sacrum (S, the part which faces towards the central sacral zone). In each of these nodes stiffness ratio (including 95 % CI) was determined. Mean stiffness ratio was determined from the obtained values and ratios for TIFI and IS were compared using Student's  $t$ -test.

The von Mises stress  $\sigma$  was also evaluated using color mapping, on the one hand, and the von Mises stress ratio %, on the other hand. Stress of both fixations was assessed in the finite elements of the model, where the highest values of the von Mises stress were observed. From collected data the von Mises stress ratio % was computed: von Mises stress ratio (TIFI) =  $\frac{\sigma_{TIFI}}{\sigma_0} \cdot 100$ , where  $\sigma_{TIFI}$  is the stress computed in the

TIFI model and  $\sigma_0$  is the stress in the model of the intact pelvis. In the case of IS, von Mises stress ratio (IS) =  $\frac{\sigma_{IS}}{\sigma_0} \cdot 100$ , where  $\sigma_{IS}$  indicates stress in

the IS model. The ratios were calculated for all data from 250 to 500 N load and the average value was computed.

### 2.3. Statistical analysis

Stiffness ratio % and the von Mises ratio % between the models of *TIFI* and *IS* were compared using Student's *t*-test and *F*-test for variance,  $p < 0.05$  was considered significant. Partial displacement of *x*, *y* and *z* axes was evaluated categorically as higher and lower displacement wherein differences of proportional representation of the higher and lower displacement were compared by Fisher's exact test, significant difference was in the case of  $p < 0.05$ .

## 3. Results

When evaluating the displacement magnitude, the mean stiffness ratio in the model of *TIFI* on the lateral fracture line (F) was 75.22% (95% CI 74.05–76.39), while in the *IS* model only 46.54% (95% CI 46.47–46.61). These differences are highly significant ( $p = 0.00005$ ). The data are shown in Table 1

and in the graphs of Fig. 2. (Mag1 corresponds to the S1 foramen, Mag2 to the S2, Mag3 to the S3 foramen and Mag4 to the S4 foramen). Table 1 shows also decreasing stiffness in the cranial-caudal direction (the highest rigidity in fixation of both S1 foramen, while the lowest at the bottom of the foramen S4). Average stiffness ratio in the medial area of the fracture line (S) in *TIFI* was 57.88% (95% CI 57.29–58.46), in *IS* only 44.74% (95% CI 44.63–44.84). These differences were also statistically significant ( $p = 0.03996$ ). The results of stiffness ratio show a higher stiffness of *TIFI* construct compared with two *IS* in transforaminal fracture. Individual calculated data are shown in Table 2 and the graphs of Fig. 3.

Partial displacement in *x*-direction was lower in the *TIFI* model than *IS* in six graphs, the differences were not statistically significant ( $p = 0.34694$ ). Conversely, in the case of partial displacements in *y*-axis direction in all nine graphs in the *TIFI* model had lower partial displacement than in the *IS* one, which was very significant ( $p = 0.00004$ ). Lower displacement in 5 graphs was shown in the *IS* model in the case

Table 1. Stiffness ratio % in fracture

Stiffness ratio %	<i>TIFI</i>	95% CI		<i>IS</i>	95%CI	
Mag1-F	80.71	79.77	81.64	51.59	51.49	51.70
Mag2-F	76.02	74.91	77.12	46.94	46.88	47.00
Mag3-F	72.89	71.68	74.09	44.59	44.56	44.63
Mag4-F	71.26	69.82	72.69	43.03	42.95	43.11
Mean	75.22	74.05	76.39	46.54	46.47	46.61
Standard deviation	3.60032	3.77451	3.42831	3.23219	3.21625	3.24829
<i>p</i> ( <i>F</i> test)	0.86346		0.79879		0.93142	
<i>p</i> ( <i>t</i> -test)	0.00005		0.00007		0.00003	

Table 2. Stiffness ratio % in the sacrum

Stiffness ratio %	<i>TIFI</i>	95% CI		<i>IS</i>	95% CI	
Mag-B	71.71	70.86	72.55	59.68	59.49	59.87
Mag1-S	59.19	58.31	60.08	44.43	44.27	44.60
Mag2-S	55.04	54.58	55.51	42.09	42.02	42.17
Mag3-S	53.47	53.12	53.82	40.04	40.00	40.09
Mag4-S	49.97	49.58	50.36	37.45	37.39	37.50
Mean	57.88	57.29	58.46	44.74	44.63	44.84
Standard deviation	7.52241	7.34116	7.70621	7.81778	7.76795	7.86768
<i>p</i> ( <i>F</i> -test)	0.94229		0.91542		0.96890	
<i>p</i> ( <i>t</i> -test)	0.03996		0.04538		0.03850	

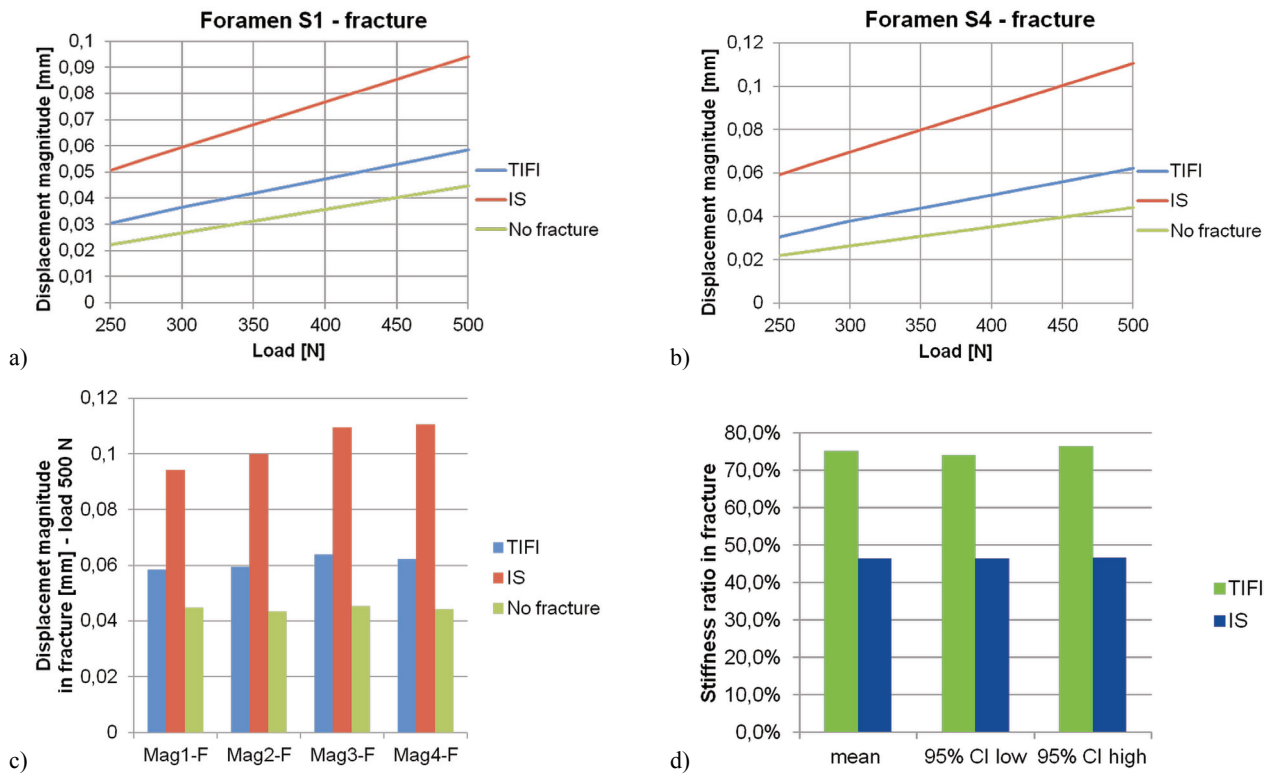


Fig. 2. Displacement magnitude in fracture: (a) displacement magnitude in fracture – foramen S1, (b) displacement magnitude in fracture – foramen S4, (c) comparison of displacement magnitudes in fracture – load 500 N, (d) Stiffness ratio comparison in fracture

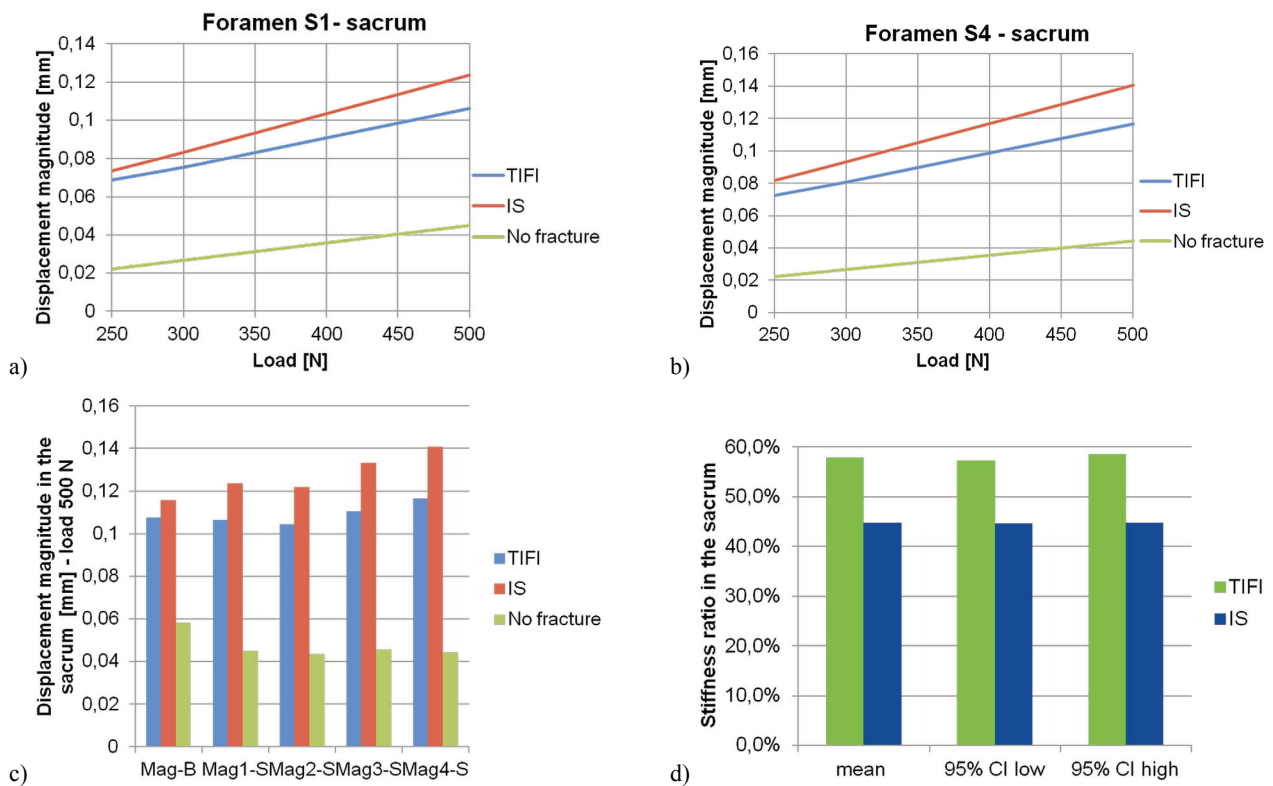


Fig. 3. Displacement magnitude in the sacrum: (a) displacement magnitude in the sacrum– foramen S1, (b) displacement magnitude in the sacrum – foramen S4, (c) comparison of displacement magnitudes in the sacrum – load 500 N, (d) stiffness ratio comparison in the sacrum

of partial displacement in the direction of  $z$ -axis ( $p = 1.00000$ ). The average von Mises stress ratio in the sacral base was 139.27% (range from 136.81 to 146.82) for *TIFI* model, for *IS* one the ratio was 565.35% (range from 470.57 to 721.92), this difference was very highly significant ( $p < 0.00001$ ). Data are shown in Table 3, respectively in the graphs of Fig. 4.

Table 3. The von Mises stress ratio %

The von Mises stress ratio %	<i>TIFI</i>	<i>IS</i>
Mean	139.27	565.35
Minimum	136.81	470.57
Maximum	146.82	721.92
Standard deviation	2.59	76.47
Student <i>t</i> -test	$p < 0.00001$	

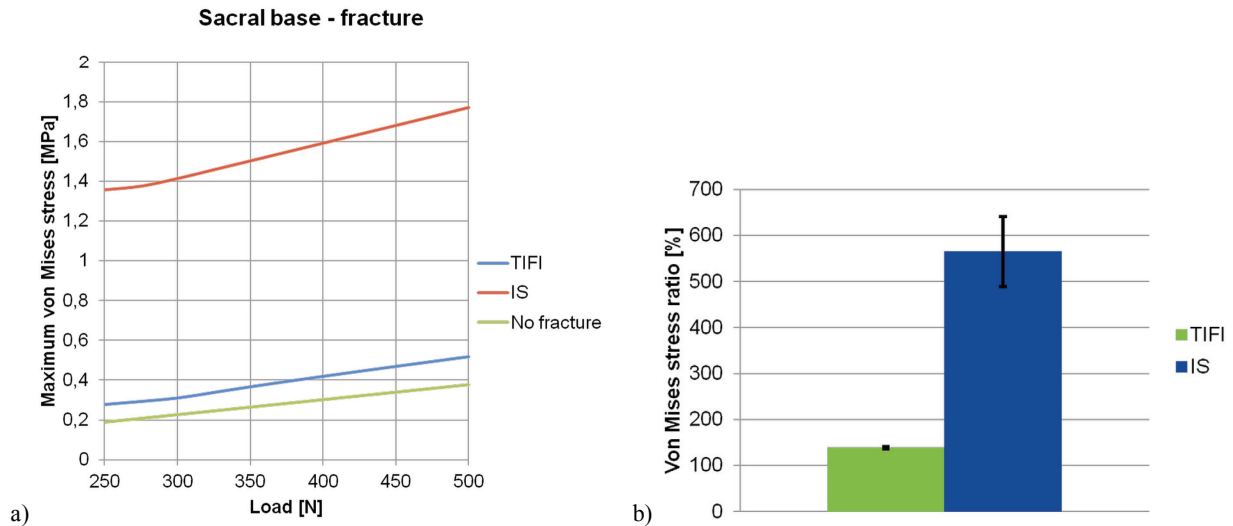


Fig. 4. The von Mises stress ratio %: (a) the von Mises stress ratio % comparison, (b) dependence of the von Mises stress on load

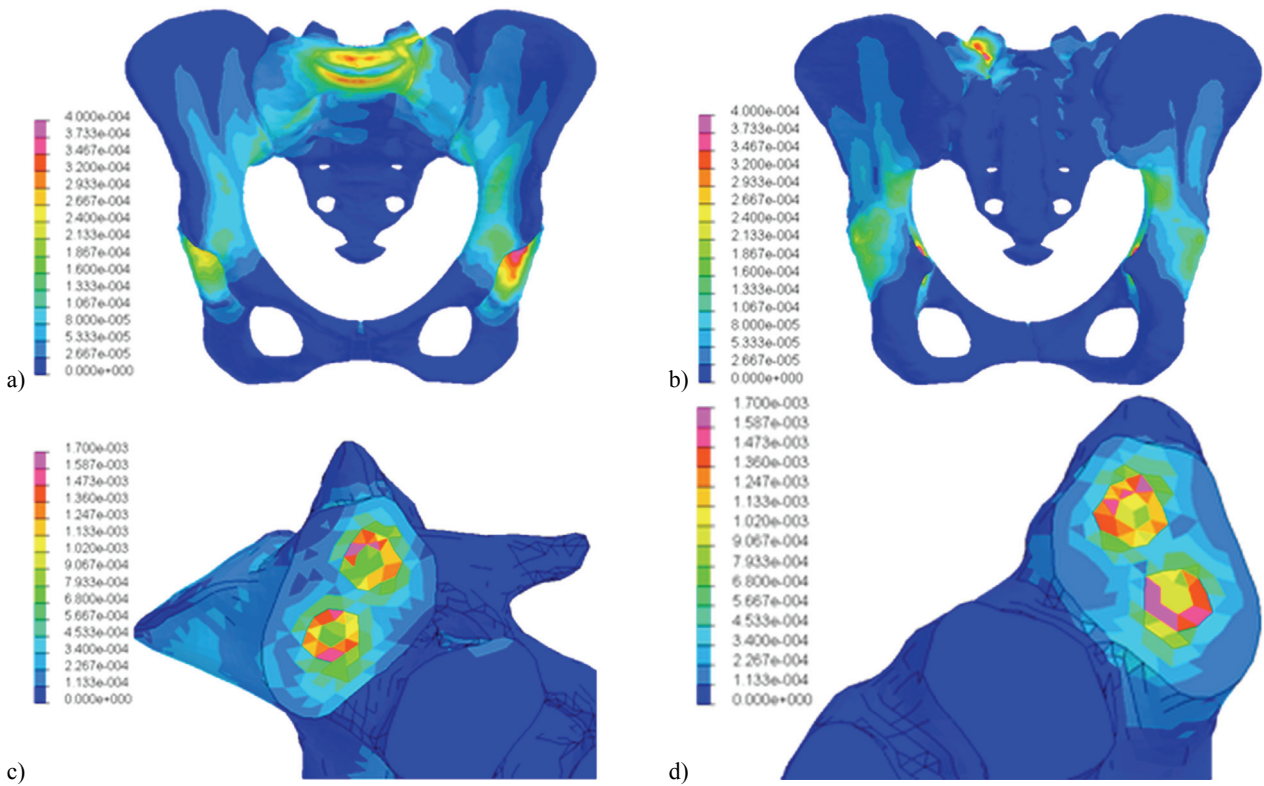


Fig. 5. The von Mises stress in the pelvis under 500 N load on sacral base [GPa], two iliosacral screws – anterior (a) and posterior view (b), The von Mises stress in sacrum in area of fracture under 500 N load on sacral base [GPa], two iliosacral screws, lateral view in fracture line – medial aspect of fracture line (c), lateral aspect of fracture line (d)



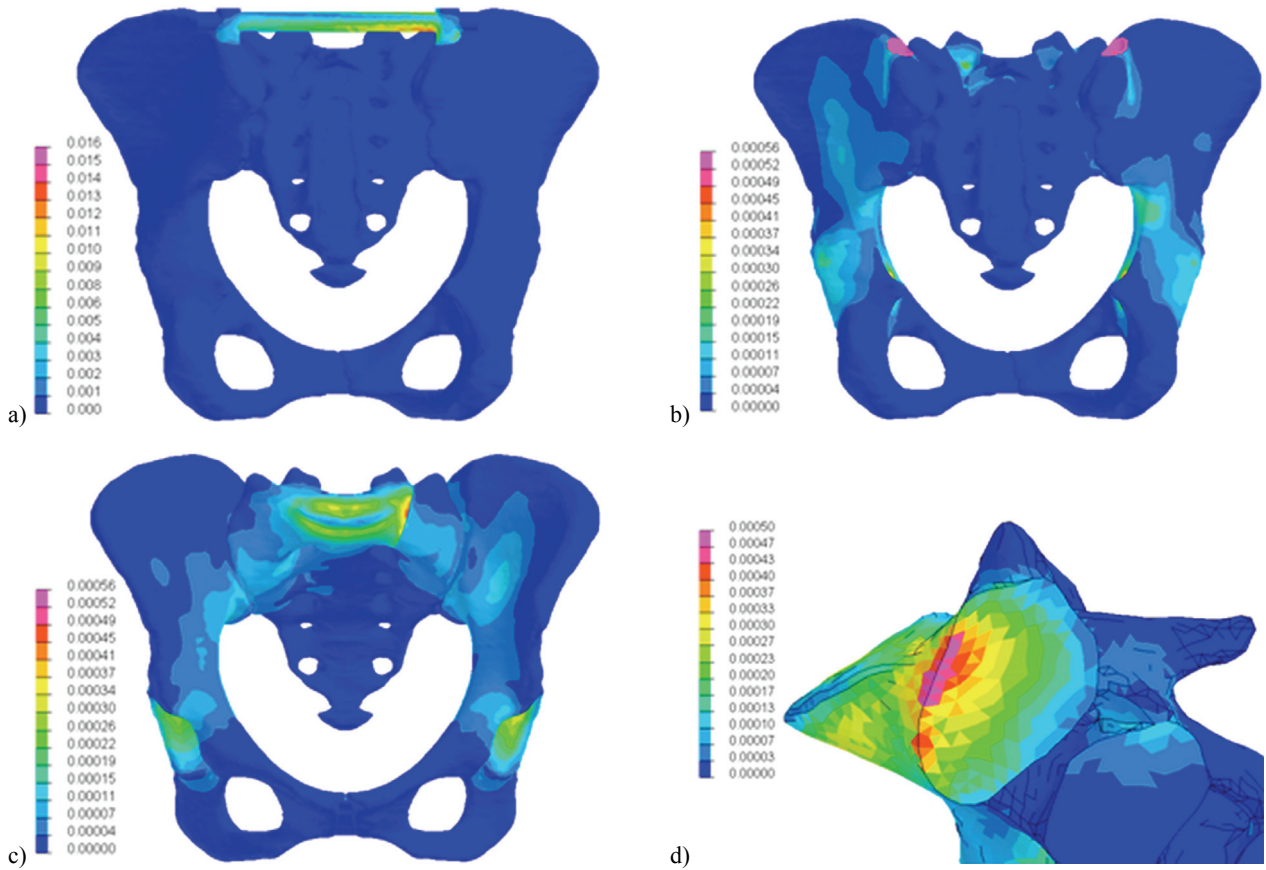


Fig. 6. The von Mises stress in the pelvis with (a) and without visualised TIFI (b) under 500 N load on sacral base [GPa] – view from back. The von Mises stress in the pelvis without visualised TIFI under 500 N load on sacral base [GPa] – front view (c), lateral view (d)

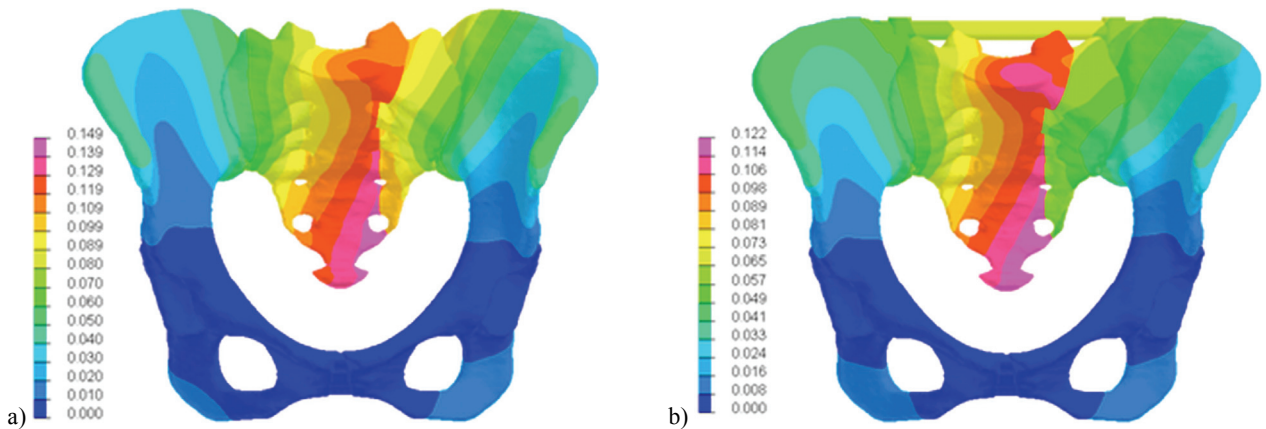


Fig. 7. Displacement magnitude in mm in the tissue under 500 N load on sacral base [mm], two iliosacral screws (a) and TIFI (b), both in front view

The results are also given in the form of colour-mapping – the von Mises stress (Fig. 5a, b and Fig. 6 a, b) and displacement (Fig. 7), the model of intact pelvis (Fig. 8). All colour maps are scaled in mm for displacement, respectively in GPa for the von Mises stress, the lowest value are blue, the highest values are violet.

During the evaluation of colour mapping insignificant vertical shift was seen in TIFI, while in the model of IS compression in the cranial part of the line was proved and distraction of the caudal part of the transforaminal fracture line, the highest compression was located in the foramen S1. The anterior-posterior displacement *TIFI* colour mapping (Fig. 7b) revealed an

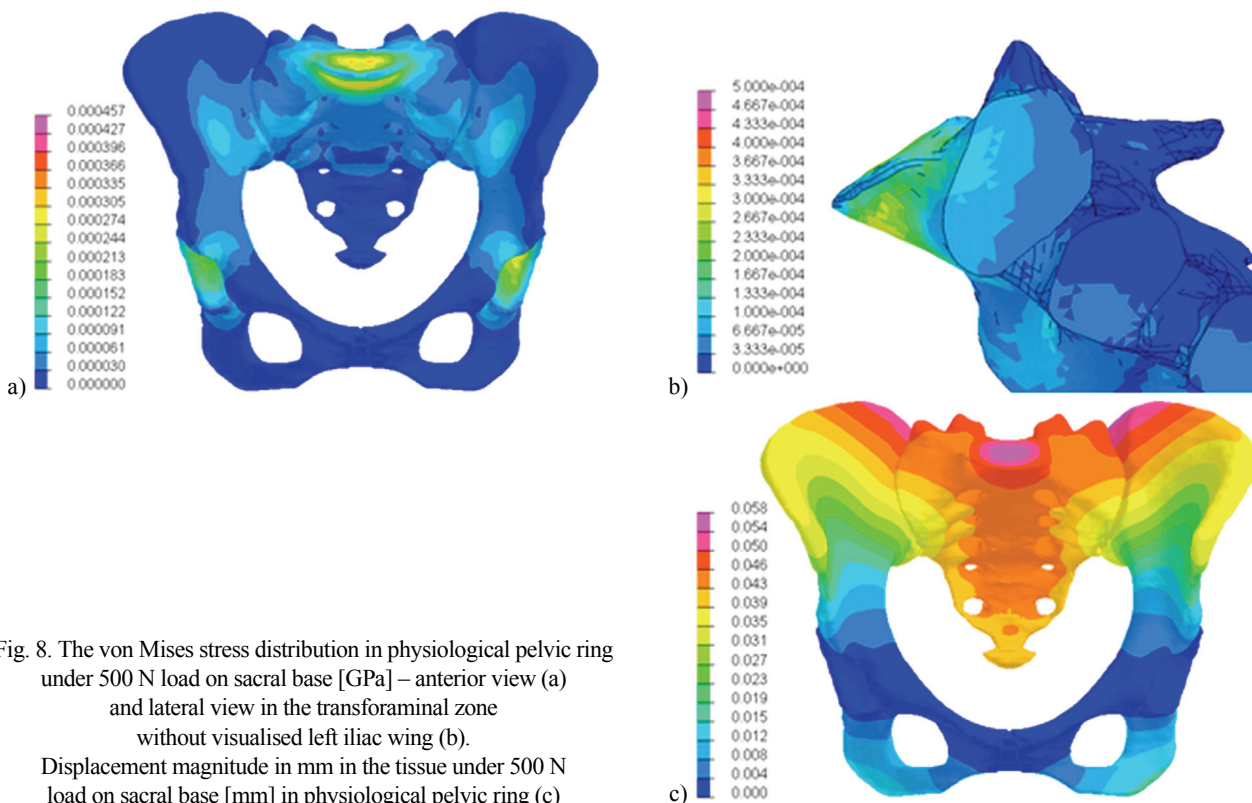


Fig. 8. The von Mises stress distribution in physiological pelvic ring under 500 N load on sacral base [GPa] – anterior view (a) and lateral view in the transforaminal zone without visualised left iliac wing (b). Displacement magnitude in mm in the tissue under 500 N load on sacral base [mm] in physiological pelvic ring (c)

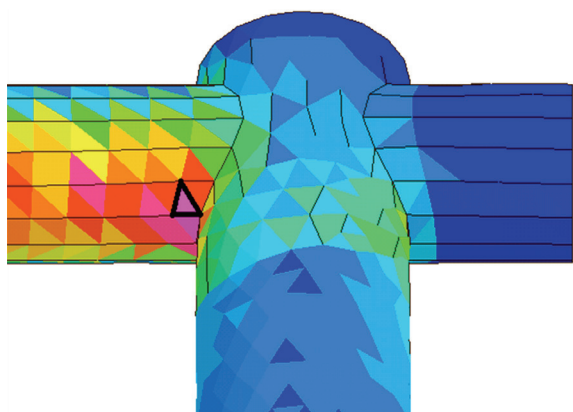


Fig. 9. Detail of the von Mises stress distribution in TIFI

increased shift in the sacral base, in the caudal part of the sacrum and in the sacrococcygeal junction. The peak displacement was situated in the caudal end of transforaminal line (shown in purple). Colour mapping of *IS* displacement in the sagittal projection shows again increased displacement zone in the sacral base, where in comparison with *TIFI* compression is higher, as in the caudal part of the sacrum, with the maximum in paracoccygeal region (violet-coloured zone, Fig. 7a).

Colour mapping of the von Mises stress on both models showed an increased stress in the sacral base, which is evident in the anterior projection (Fig. 6c, Fig. 6a). Different spatial distribution of stress has been shown in lateral projections, the maximum bone

stress of *TIFI* is located in the ventral part of the segment S1, near the base on the medial surface of the fracture line (Fig 6d), whereas in the case of *IS* the maximum stress is reached in the central part of the segment S1, in the immediate vicinity of the two screws (Fig. 5c, 5d), the peak stress is on the lateral fracture line, near the caudally placed screw (purple area, Fig. 5d). Extraosseous stress was computed only in the *TIFI* model. The peak stress was shown in the connecting rod near the medial edge of the head of screw contra-laterally to the fracture (Fig. 9).

## 4. Discussion

Biomechanics of TIFI was first described by Dienstknecht et al. in 2011, who measured displacement on cadaverous pelvises [4]. Injury 61-C1.2 was simulated (complete disruption of the sacroiliac and complete symphyseolysis). The disrupted dorsal segment was stabilized gradually with these implants: 1. two three-hole dynamic, 4.5 compression plates (Synthes<sup>®</sup>), 2. two 6.5 mm cannulated partially threaded screws (Synthes<sup>®</sup>), 3. the transiliac internal fixator (USS) with 6-mm diameter screws and a 5-mm diameter connection rod. A four-hole AO dynamic compression plate was used for fixation of symphyseolysis.



The stabilized pelvis was loaded in the L5 vertebra, the load was neutralized on the model of the femoral head (acetabulum was simulated using an implanted polyethylene hip prosthesis cup; the diameter of the mounted head was 28 mm). Statistically insignificant differences were found between fixations, when the shifts in the direction of  $x$  and  $y$  axes were compared. Displacement movements in  $z$ -axis (vertical displacement motion) were significantly lower in the *TIFI* construct than 2 *IS* or 2 plates, vertical displacement of *TIFI* was comparable with the intact pelvis. A finite element analysis has not been performed in this study, neither have the results of comparative studies on a plastic model been included (according to the methodology used for comparing the initial measurement to the anatomical model). Although intact ligamentous structures were described, densitometric analysis of the specimen was not listed (DXA, respectively quantitative CT densitometry), therefore physiological bone structure of the specimens was not confirmed. Sacral fractures fixation was not included in this study.

Chen et al. [10] conducted research on biomechanics of minimally invasive fixation in stabilizing the vertical unstable fractures of the sacrum (type 61-C1.3). Their work is focused on modelling unilateral sacral fractures in the transalar, transforaminal and central zone (Denis I, II and III fracture). The research was performed in two parts: a clinical and biomechanical one. Iliosacral screws, as well as a transiliac plate (3.5 pelvic reconstruction plate) were used for fixation of fractures. Clinical results of both types of fixation regardless of the type of fracture did not differ significantly. The biomechanical study was performed on the finite element model of the pelvic ring, which was created from CT and MRI scans of the intact pelvis. The computation loads and boundary conditions of two groups of FE models referred to the balance-standing phase of the intact pelvis model. The compressive state implemented a 500 N vertical load; the flexion state implemented a 500 N vertical load and a 10 Nm moment of forward sagittal direction; the lateral bending state implemented a 500 N vertical load and a 10 Nm moment of right lateral direction.

In the FE model used, percutaneous plate fixation was superior to percutaneous iliosacral screw fixation for the treatment of Denis III type vertical sacral fractures, while in the case of fixation of fractures in the transalar (Denis I type) and transforaminal zone (Denis II type) no significant differences were found between the transiliac plate and two *IS* [10]. Biome-

chanics of a 4.5 transiliac plate was described by Bodzay et al. [2]. Their study was performed on an anatomical model. Injury 61-C1.3 was modelled as complete transalar fracture (Denis I type), complete symphyseolysis was made in the anterior segment. The posterior pelvic segment was stabilized gradually with two three-hole reconstruction plates being used, positioned at 60–90 degrees to each other on the linea terminalis, or with a narrow dynamic compression plate (10–12 hole 4.5 DC plate). The anterior segment was stabilized with a four-hole narrow dynamic compression (DC) plate (placed on the cranial aspect of the symphysis).

The load was transferred to the vertebra L5 and neutralized in the ipsilateral proximal femur that has been held fixed. Displacement movements were measured by extensometer placed on the front surface of the sacral fracture line. There was simulated unilateral cyclic load during walking (vertical load from 100 to 250 N), which corresponds to a partial weight bearing at the beginning of postoperative mobilization. 1000 cycles with 1 Hz were performed. The ANOVA test did not reveal statistically significant differences in the case of displacement between the transiliac plate and 2 anterior reconstruction plates. Our study describes first the analysis of displacement and the von Mises stress of the transiliac internal fixator in the finite element (FE) model. The advantage of FE analysis is the possibility of calculating the stress and the total and partial displacements for selected values of the load, and in selected areas of the model. Moreover, it is possible to evaluate separately the medial and lateral surface of the fracture line. Unlike the above study by Dienstknecht et al. [4], in which significant differences only in partial vertical displacement ( $z$ -axis) were shown, the current study demonstrates the significant differences in the total displacement in the whole transforaminal zone, regardless of the surface of the fracture line, as in the case of partial displacements in the  $y$ -direction. Conversely, comparison of partial displacements in the direction of  $x$  and  $z$  axes revealed no significant differences. Biomechanics of *TIFI* and the transiliac plate allows also only indirect comparisons, although the connecting rod is analogous to the plate. The insertion of standard or locking screws in the plate is different from the polyaxial screw, so there can be supposed different biomechanical properties. However, direct biomechanical comparison of *TIFI* and the transiliac plate has not been performed in any study.

Comparison of the spatial distribution of stress in *TIFI* is not included in either of the above-

mentioned studies. Significantly higher stress was proved in the model of *IS* in comparison with *TIFI* in fixation of transforaminal fracture. Chen et al. [10] in above-mentioned study also demonstrated the increasing stress in the lateral–medial direction in the model of *IS* (from transalar fracture, where the minimum stress is, to the central fracture, where the peak stress is).

The over-compression of iliosacral screws can be prevented by the use of fully threaded screws, but these screws are coupled with a decrease of intra-operative reduction range. Also partially threaded screws could be used with lesser compression in the case of insertion of threaded part of these screws around the fracture line, but this insertion is technically very demanding and could be performed only by very experienced pelvic surgeon.

Implantation of *TIFI* is technically easier than in the case of iliosacral screwing and without a higher risk of the over-compression. Both *TIFI* and iliosacral screw stabilization can be performed in the acute period of treatment, but *TIFI* is inserted only in a prone position, which can limit or prevent the use in the case of associated severe thoracic and abdominal trauma. For these polytraumatized patients with contraindication for prone position the pelvic surgeon has some options of urgent stabilization: ap pelvic C clamp (also connected with higher risk of the over-compression of transforaminal zone), a pelvic external fixator (addressed to the iliac wing in the emergent phase, external fixation is connected with lower stability than the C clamp) and the iliosacral screw (in emergency, only one screw is inserted in injured side of posterior segment).

## 5. Conclusion

Both *TIFI* and *IS* provide sufficient stiffness for minimally invasive stabilization of unstable transforaminal fractures. However, data from the FE analysis showed a significantly higher stiffness of *TIFI* and lower stress in the first sacral segment, so there is the lower the risk of over compression of the fracture line in comparison with two *IS*. *TIFI* is biomechanically superior to two *IS* for treatment of transforaminal fractures (Denis II type), especially for comminutive fractures, because excessive compression of the comminutive zone might cause iatrogenic damage to the sacral nerve roots. Biomechanical superiority of *TIFI* will need to be confirmed in a prospective comparative clinical study.

## Acknowledgements

This work was supported by the European Regional Development Fund (ERDF), project European Centre of Excellence, NTIS – New Technologies for Information Society, CZ.1.05/1.1.00/02.0090 and by the grant SVV 2014 No. 260 052.

All authors would like to thank assistant. Ing. Luboš Lobovský, Ph.D. for the full development of the original analytical software for contactless stereo-photometric system, that had been used for displacement measurement in the plastic model of the pelvis.

## References

- [1] BODZAY T., FLÓRIS I., VÁRADI K., *Comparison of stability in the operative treatment of pelvic injuries in a finite element model*, Arch. Orthop. Trauma Surg., 2011, 131(10), 1427–1433.
- [2] BODZAY T., SZITA J., MANÓ S., KISS L., JÓNÁS Z., FRENÝÓ S., CSERNÁTONY Z., *Biomechanical comparison of two stabilization techniques for unstable sacral fractures*, J. Orthop. Sci., 2012, 17(5), 574–579.
- [3] DIENSTKNECHT T., BERNER A., LENICH A., NERLICH M., FUECHTMEIER B., *A Minimally invasive stabilizing system for dorsal pelvic ring Injuries*, Clin. Orthop. Relat. Res., 2011, 469(11), 3209–3217.
- [4] DIENSTKNECHT T., BERNER A., LENICH A., ZELLNER J., MUELLER M., NERLICH M., FUECHTMEIER B., *Biomechanical analysis of a transiliac internal fixator*, Int. Orthop, 2011, 35(12), 1863–1868.
- [5] DŽUPA V., PAVELKA T., TALLER S. et al., *Léčbazloženin-pánve a acetabula*, Galén 2013.
- [6] FÜCHTMEIER B., MAGHSUDI M., NEUMANN C., HENTE R., ROLL C., NERLICH M., *The minimally invasive stabilization of the dorsal pelvic ring with the transiliacal internal fixator (TIFI) – surgical technique and first clinical findings*, Unfallchirurg, 2004, 107, 42–51.
- [7] GRAS F., MARINTSCHEV I., WILHARM A., KLOS K., MÜCKLEY T., HOFMANN G.O., *2D-fluoroscopic navigated percutaneous screw fixation of pelvic ring injuries a case series*, BMC Musculoskelet. Disord., 2010, 11, 153.
- [8] HAO T., CHANGWEI Y., QIULIN Z., *Treatment of posterior pelvic ring injuries with minimally invasive percutaneous plate osteoSynthes©is*, Int. Orthop., 2009, 33, 1435–1439.
- [9] CHEN B., ZHANG Y., XIAO S., GU P., LIN X., *Personalized image-based templates for iliosacral screw insertions: a pilot study*, Int. J. Med. Robot., 2012, 8(4), 476–482.
- [10] CHEN H., WU L., ZHENG R., LIU Y., LI Y., DING Z., *Parallel analysis of finite element model controlled trial and retrospective case control study on percutaneous internal fixation for vertical sacral fractures*, BMC Musculoskelet. Disord., 2013, 14, 217.
- [11] CHEN W., HOU Z., SU Y., SMITH W.R., LIPORACE F.A., ZHANG Y., *Treatment of posterior pelvic ring disruptions using a minimally invasive adjustable plate*, Injury, 2013, 44(7), 975–980.
- [12] MENDEL T., KUHN P., WOHLRAB D., BREHME K., *Minimal-invasive Stabilisierung einer bilateralen Sakrumfraktur mit lumbopelviner Dissoziation*, Unfallchirurg, 2009, 112, 590–595.
- [13] POHLEMANN T., GÄNSSLEN A., SCHELLWALD O., CULEMANN U., TSCHERNE H., *Outcome after pelvic ring injuries*, Injury, 1996, 27 (Suppl. 2), 31–38.

- [14] REILLY M.C., BONO C.M., LITKOUHI B., SIRKIN M., BEHRENS F.F., *The effect of sacral fracture malreduction on the safe placement of iliosacral screws*, J. Orthop. Trauma, 2003, 17(2), 88–94.
- [15] ROSENBERGER R.E., DOLATI B., LARNDORFER R., BLAUTH M., KRAPPINGER D., BALE R.J., *Accuracy of minimally invasive navigated acetabular and iliosacral fracture stabilization using a targeting and noninvasive registration device*, Arch. Orthop. Trauma Surg., 2010, 130, 223–230.
- [16] ROWE S.A., SOCHOR M.S., STAPLES K.S., WAHL W.L., WANG S.C., *Pelvic ring fractures: Implications of vehicle design, crash type and occupant characteristics*, Surgery, 2004, 136, 842–847.
- [17] TALLER S., ŠRÁM J., *Pakloubpo longitudinální zlomenině centrální zónysakra s kónickou instabilitou pánevní hokruhu*, Acta Chir. Orthop. Traum. Čech, 2011, 78, 82–85.
- [18] TOSOUNIDIS G., CULEMANN U., WIRBEL R., HOLSTEIN J.H., POHLEMANN T., *Die perkutane transiliosakrale Zugschrauben osteoSynthes®e des hinteren Beckenrings (Erhöhte Sicherheit durch Standardisierung von Visualisierung und Technik)*, Unfallchirurg, 2007, 110, 669–674.
- [19] VAN ZWIENEN C.M., VAN DEN BOSCH E.W., SNIJDERS C.J., KLEINRENSINK G.J., VAN VUGT A.B., *Biomechanical Comparison of Sacroiliac Screw Techniques for Unstable Pelvic Ring Fractures*, J. Orthop. Trauma, 2004, 18, 589–595.
- [20] ZHENG Z., ZHANG Y., HOU Z., HAO J., ZHAI F., SU Y., PAN J., *The application of a computer-assisted thermoplastic membrane navigation system in screw fixation of the sacroiliac joint – A clinical study*, Injury, 2012, 43(4), 495–499.
- [21] ZWINGMANN J., HAUSCHILD O., BODE G., SÜDKAMP N.P., SCHMAL H., *Malposition and revision rates of different imaging modalities for percutaneous iliosacral screw fixation following pelvic fractures: a systematic review and meta-analysis*, Arch. Orthop. Trauma Surg., 2013, 133(9), 1257–1265.